Modulating the Magnetic Properties of Copper(II)/Nitroxyl Heterospin Complexes by Suppression of the Jahn-Teller Distortion

Sam Greatorex, Sergey V. Fokin, Rafal Kulmaczewski, Mihoko Yamada, Oscar Cespedes, Nobuto Yoshinari, Takumi Konno, Stephen Sproules,* Victor I. Ovcharenko,* and Malcolm A. Halcrow*

ABSTRACT: A series of six-coordinate $[Cu(L)L^1][BF_4]_2$ (L^1 = 2,6-*bis*{1-oxyl-4,4,5,5-tetramethyl-4,5-dihydro-1*H*-imidazol-2-yl}pyridine) complexes is reported. Ferromagnetic coupling between the Cu and L^1 ligand spins is enhanced by a 'L' co-ligand with distal methyl substituents, which is attributed to a sterically-induced suppression of its Jahn-Teller distortion.

Jahn-Teller distortions of Cu(II) complexes of meridional tridentate ligands can be unusually plastic.[1-5] Such compounds usually exhibit Jahn-Teller elongated structures with a $\{d_{x^2-y^2}\}^1$ electron configuration (structure A, Chart 1),[6] which may interconvert with the isomeric structure A' if their two ligands are identical,[7] such as in salts of $[Cu(terpy)_2]^{2+}$.[8] However, this is transformed to an alternative $\{d_{z^2}\}^1$ ground state (structure B) by ligands promoting lengthening of *all* the distal Cu–N bonds.[9] This can be driven by steric crowding,[2,3] conformational strain[3] or reduced basicity of the distal N-donor atoms.[4] One such compound transforms from structure B towards structure A on cooling, which is coupled to anion disorder in the crystal.[4]

In another context, flexible Jahn-Teller distortions can afford switchable molecular materials in copper(II) complexes of nitroxyl radical ligands.[1,10] Thermal, light- or pressure-induced reorientation of their Jahn-Teller elongation axis flips the metal $d_{x^2-y^2}$ magnetic orbital, changing the magnitude and sign of the metal-radical interaction. That causes large changes in the color, magnetic moment and EPR spectrum of the material. This phenomenon is best studied in $[Cu(hfac)_2]$/nitronyl nitroxide coordination polymers,[11] but molecular complexes of chelating nitroxyl ligands can also exhibit the effect.[12]

With this in mind, we targeted the heteroleptic complexes $[Cu(L)L^1]^{2+}$, where L^1 is the biradical 2,6-*bis*{1-oxyl-4,4,5,5-tetramethyl-4,5-dihydro-1*H*-imidazol-2-yl}pyridine[13-18] and L is another tridentate ligand (Charts 2 and S1). The steric influence of the L^1 methyl substituents should promote a Jahn-Teller elongation along the Cu–iminonitroxyl (IMNT) bonds (structure A). However, introducing comparable steric bulk to the L co-ligand might perturb the Jahn-Teller properties of the complex,[2,3] either by changing the axis of elongation (structure A') or inducing a transformation to structure B. This would perturb the magnetic properties of the molecule, which could afford a new type of switchable magnetic solid. Magnetic exchange between Cu(II) ions and coordinated IMNT radicals is usually ferromagnetic in character, but is 10x smaller when the radical occupies an axial[19,20] rather than an equatorial site[16,20-22] in a tetragonal Cu(II) complex.

Chart 1 Jahn-Teller isomers of the complexes in this work.[6,9] Short and long Cu–N bonds are indicated by full and dotted lines, respectively. The red ligand in each molecule represents the 'L' co-ligand (Chart 2).

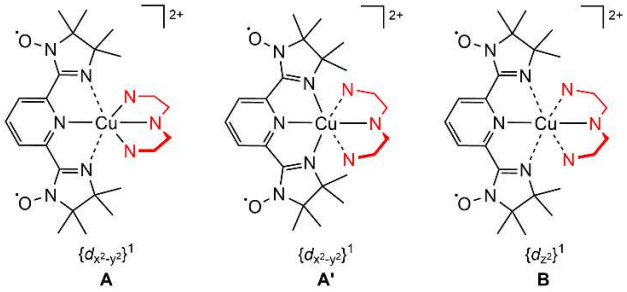

Chart 2 The ligands and complexes employed in this work.

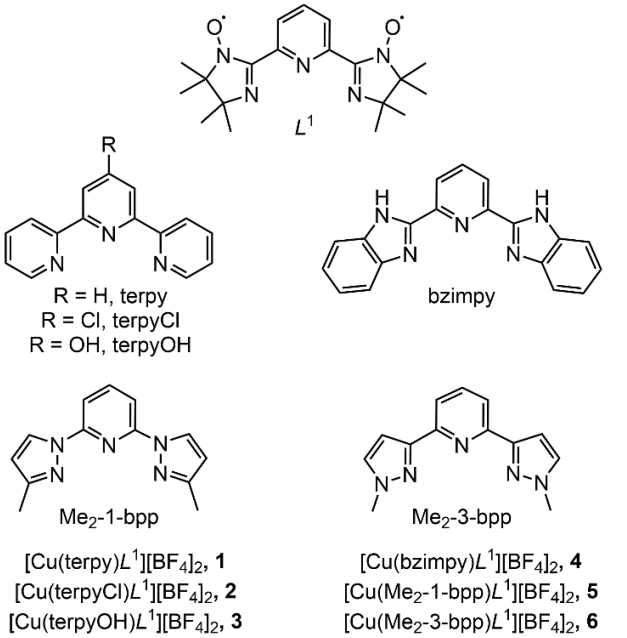

$[Cu(terpy)L^1][BF_4]_2$, **1**
$[Cu(terpyCl)L^1][BF_4]_2$, **2**
$[Cu(terpyOH)L^1][BF_4]_2$, **3**
$[Cu(bzimpy)L^1][BF_4]_2$, **4**
$[Cu(Me_2\text{-}1\text{-}bpp)L^1][BF_4]_2$, **5**
$[Cu(Me_2\text{-}3\text{-}bpp)L^1][BF_4]_2$, **6**

Reaction of equimolar quantities of $Cu[BF_4]_2{\cdot}6H_2O$, L^1 and the appropriate co-ligand (L) in methanol gave $[Cu(L)L^1][BF_4]_2$ as dark red precipitates (Chart 1). Their formulations were confirmed by mass spectrometry and microanalysis, with **3**, **4** and **6** containing one or two equiv lattice water. Their stability may reflect the steric influence of the L^1 α-methyl substituents, which would inhibit the formation of $[Cu(L^1)_2]^{2+}$ by ligand exchange. The compounds form clusters of plate-like crystals from common solvents, which are often deliquescent. Hence only one example was crystallographically characterized, namely $\mathbf{2}{\cdot}n MeNO_2$ ($n \approx 2.1$). While the refinement suffers from disorder (Figures S5 and S6), the main features of the structure are clear (Figure 1). The complex adopts structure A (Chart 1), with a Jahn-Teller elongation to the distal N-donors of the L^1 ligand [Cu(1)–N(9) = 2.289(5) and Cu(1)–N(19) = 2.323(5) Å].

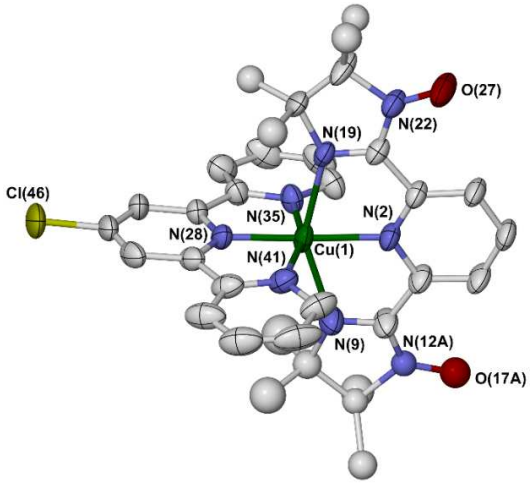

Figure 1 The $[Cu(terpyCl)L^1]^{2+}$ cation in $\mathbf{2}{\cdot}n MeNO_2$. Only one orientation of the disordered L^1 ligand atoms is shown, H atoms are omitted and displacement ellipsoids are at the 50 % level. Color code: C, white; Cl, yellow; Cu, green; N, blue; O, red.

The complexes exhibit $\chi_M T$ = 1.20-1.33 $cm^3mol^{-1}K$ at room temperature, close to the value predicted by the Curie law for three weakly interacting S = ½ spins.[23] $\chi_M T$ for all the compounds increases upon cooling, implying the presence of ferromagnetic exchange interactions, although the rate of increase varies between the samples (Figures 2, S7 and S8). The data were modelled by a Hamiltonian treating exchange between the Cu (S_1) and L^1 radical spins (S_2, S_3; eq 1):[16]

$$H = -2J(S_1{\cdot}S_2 + S_1{\cdot}S_3) - 2J'(S_2{\cdot}S_3) \qquad (1)$$

where J describes the Cu···L^1 interaction and J' is the *intra*-ligand coupling between the L^1 spins (Table 1). Small decreases in $\chi_M T$ for $\mathbf{2}$-$\mathbf{4}{\cdot}H_2O$ below 10 K are not reproduced by the fits, and might reflect weak intermolecular interactions which are not included in the model. A low-temperature decrease in $\chi_M T$ for $\mathbf{6}{\cdot}2H_2O$ has no influence on its fitted parameters, though (Figure S8). Variations in g{Cu} may reflect small temperature-independent paramagnetism or paramagnetic impurity contributions to the data. However these were omitted from the analysis, since satisfactory fits were obtained without them.

Compounds **1**-**5** show ferromagnetic Cu···L^1 coupling ($+11 \le J \le +19$ cm^{-1}) and an antiferromagnetic intra-ligand interaction (Table 1). The values of J are consistent with a Jahn-Teller elongation along the Cu–N{IMNT} bonds in structure A (Chart 1), as observed crystallographically for **2**.[20] However $\mathbf{6}{\cdot}2H_2O$, with the distally methylated co-ligand Me_2-3-bpp (Chart 2), shows larger values for J (+50 cm^{-1}) and J' (−25 cm^{-1}). Hence,

Table 1 Fitted magnetic exchange parameters for the compounds in this work (Figure 2).

	g{Cu}	g{NO}	J{Cu…NO}	J'{NO…NO}	R^2
1	2.151(6)	2.01[a]	+17.4(5)	−4.6(2)	0.991
2	2.121(2)	2.01[a]	+11.6(2)	−2.8(1)	0.996
$\mathbf{3}{\cdot}2H_2O$	2.175(4)	2.01[a]	+13.5(2)	−1.0(1)	0.999
$\mathbf{4}{\cdot}H_2O$	2.102(4)	2.01[a]	+11.2(3)	−5.2(1)	0.977
5	2.111(4)	2.01[a]	+10.9(2)	−0.5(1)	0.997
$\mathbf{6}{\cdot}2H_2O$	2.082(4)	2.01[a]	+49.6(9)	−25.4(5)	0.951

[a]This value was fixed during the fitting process.

the electronic structure of **6** is different from the other complexes. The antiferromagnetic J'{NO···NO} values were reproduced computationally (see below), but contrast with free L^1 [24] and its $ZnCl_2$ adduct[16] which show ferromagnetic intra-ligand coupling. Precedent is provided by 2,6-*bis*{3-oxide-1-oxyl-4,4, 5,5-tetramethyl-4,5-dihydro-1*H*-imidazol-2-yl}pyridine (L^2), the nitronyl nitroxide analogue of L^1. J'{NO···NO} is also ferromagnetic in L^2,[25] but is antiferromagnetic in $[Cu(L^2)_2]^{2+}$.[26]

Since the materials were only available in small quantities, these results were investigated by gas phase DF calculations. Structure minimizations of $\mathbf{1}^{2+}$-$\mathbf{6}^{2+}$ (the $[Cu(L)L^1]^{2+}$ cations in **1**-**6**, Chart S2) employed the ω-B97X-D functional and 6-311G** basis set, which assigned structure A to $\mathbf{1}^{2+}$-$\mathbf{4}^{2+}$ with a Jahn-Teller elongation along the Cu–N{IMNT} bonds (Chart 1). The Cu–N distances are similar in each case, and agree well with the experimental values for **2** (Table 2). However structure A', with a Jahn-Teller elongation along the Cu–N{bpp} bonds, was the lowest energy isomer for $\mathbf{5}^{2+}$ and $\mathbf{6}^{2+}$ by this protocol. That reflects competition between the steric influence of the methyl groups on each ligand, combined with the intrinsic preference of six-coordinate copper(II) compounds for a $\{d_{x2-y2}\}^1$ ground state.[1]

The complexes were also minimized in their alternative Jahn-Teller isomer, by constraining the appropriate elongated Cu–N bonds to 2.29 Å (Table 2). The energy difference between the two isomers (ΔE) is $0.2 \le |\Delta E| \le 2.1$ kcalmol^{-1}. That is comparable to the thermal energy kT, showing the Jahn-Teller structures of $\mathbf{1}^{2+}$-$\mathbf{6}^{2+}$ in condensed phases should be strongly influenced by environmental factors such as crystal packing. That could explain why the lowest structure predicted by ΔE for $\mathbf{5}^{2+}$ and $\mathbf{6}^{2+}$ does not match that observed experimentally.

The higher energy isomer of $\mathbf{6}^{2+}$ resembles structure B (Chart 1) from its Cu–N{pyrazolyl} distances, which are 0.06 Å longer than the equivalent distances in structure A of $\mathbf{5}^{2+}$.[2-4] The highest lying metal-based α-orbital of this isomer of $\mathbf{6}^{2+}$ also has increased $\{d_{z2}\}^1$ character (Figures S10-S15). The Cu–N{pyrazolyl} distances in $\mathbf{6}^{2+}$ are consistently longer than in $\mathbf{5}^{2+}$ (Table 2), because the N–CH_3 bonds in Me_2-3-bpp (1.45 Å) are shorter than the C–CH_3 bonds in Me_2-1-bpp (1.49 Å). That places those methyl groups closer to the metal ion in $\mathbf{6}^{2+}$, giving them a greater steric influence on the coordination sphere.

J{Cu···NO} exchange constants were calculated from the DFT-minimized structures, at the M06L/ZORA-def2-TZVPP level (see Supporting Information for details). Computed J values for structure A of $\mathbf{1}^{2+}$-$\mathbf{4}^{2+}$ are +10-16 cm^{-1} (Table 2), confirming those compounds adopt structure A in the solid state (Table 1). Larger J values are computed for $\mathbf{5}^{2+}$ and $\mathbf{6}^{2+}$, with J for $\mathbf{6}^{2+}$ in structure B (40 cm^{-1}) approaching the measured value of 50 cm^{-1}. That reflects overlap of the L^1

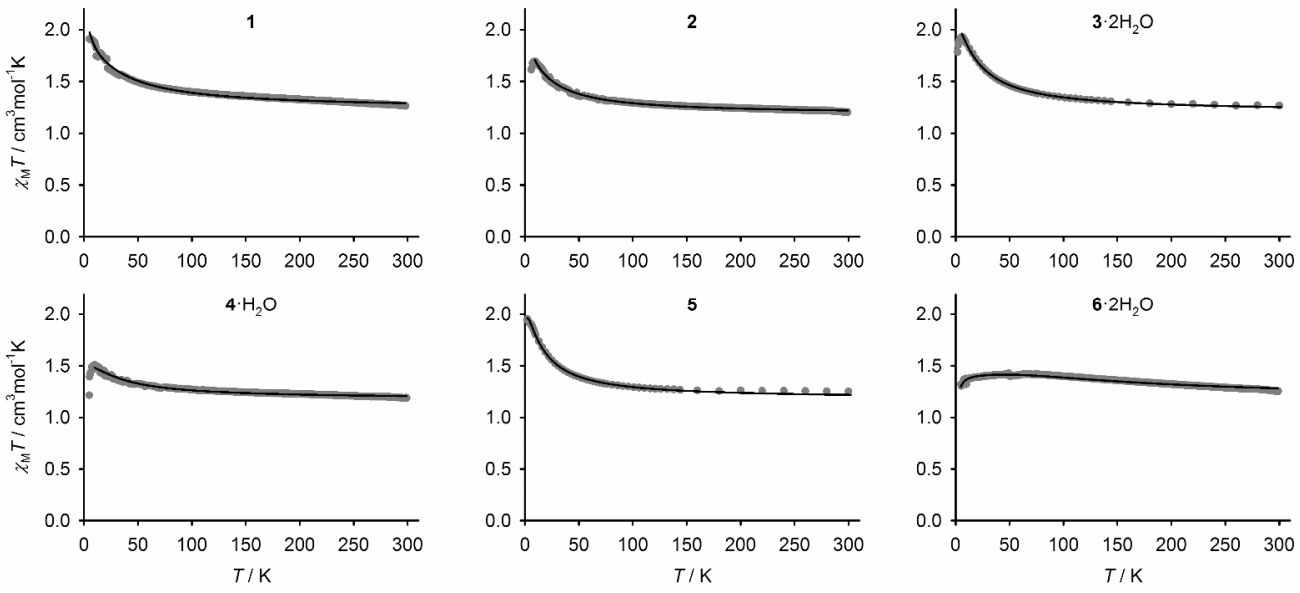

Figure 2. Measured (gray) and fitted (black) magnetic susceptibility data for the compounds in this work. Alternative curve fits to validate the results in Table 1 are in Figures S7 and S8,

Table 2 Calculated Cu–N distances (Å) and exchange coupling constants (cm^{-1}) for the energy-minimized structures of 1^{2+}-6^{2+} (Chart 1); and the energy difference between the two isomers for each compound ($kcalmol^{-1}$). Experimental data for 2·*n*$MeNO_2$ are included for comparison, while other measured *J* and *J'* values are in Table 1. A negative value of Δ*E* shows structure A or B (for 6^{2+}) is the lowest energy isomer under these conditions, and *vice versa*.

	2·*n*$MeNO_2$	$\mathbf{1}^{2+}$	$\mathbf{2}^{2+}$	$\mathbf{3}^{2+}$	$\mathbf{4}^{2+}$	$\mathbf{5}^{2+}$	$\mathbf{6}^{2+}$
	Structure A	Structure A[a]	Structure A[a]	Structure A[a]	Structure A[a]	Structure A	Structure B
Cu–N{L^1 pyridyl}	2.052(4)	2.092	2.090	2.089	2.110	2.055	2.044
Cu–N{L^1 IMNT}	2.289(5), 2.323(5)	2.290, 2.290	2.288, 2.288	2.287, 2.291	2.288, 2.288	2.290, 2.290[b]	2.290, 2.290[b]
Cu–N{L pyridyl}	1.943(4)	1.971	1.968	1.963	2.025	1.991	1.989
Cu–N{L distal}	2.062(5), 2.064(4)	2.090, 2.091	2.093, 2.095	2.096, 2.102	2.061, 2.062	2.106, 2.106	2.161, 2.166
J{Cu···NO}	+11.6	+13.6	+14.5	+15.8	+9.8	+23.7	+39.7
		Structure A'	Structure A'	Structure A'	Structure A'	Structure A'[a]	Structure A'[a]
Cu–N{L^1 pyridyl}	–	2.005	2.004	2.006	2.006	2.007	2.003
Cu–N{L^1 IMNT}	–	2.129, 2.129	2.128, 2.128	2.134, 2.135	2.102, 2.102	2.088, 2.088	2.119, 2.119
Cu–N{L pyridyl}	–	2.027	2.024	2.011	2.096	2.108	2.027
Cu–N{L distal}	–	2.290, 2.290[b]	2.290, 2.290[b]	2.290, 2.290[b]	2.290, 2.290[b]	2.263, 2.272	2.295, 2.311
J{Cu···NO}	–	+108.6	+109.6	+104.8	+126.5	+136.4	+115.1
J'{NO···NO}	−2.8	−3.5	−3.2	−3.1	−2.1	−6.0	−4.4
Δ*E*	–	–0.9	–0.5	–0.9	–0.2	+1.5	+2.1

[a]This is the lowest energy isomer computed for this compound in the gas phase. [b]This value was fixed during the minimization of the higher energy Jahn-Teller isomer.

N{IMNT} donor atoms with the SOMO d_{z2} orbital torus, leading to a significantly larger Cu *d* contribution to the L^1 SOMO in $\mathbf{5}^{2+}$ and $\mathbf{6}^{2+}$ (Figure S15, Table S6).[21] All the complexes gave *J* >100 cm^{-1} in the alternative A' isomer, which is inconsistent with observation and confirms none of the compounds adopt that structure.

J'{NO···NO} for $\mathbf{1}^{2+}$-$\mathbf{6}^{2+}$ was also calculated, using the corresponding $[Zn(L)L^1]^{2+}$ complexes as models. These were weakly antiferromagnetic as observed experimentally, although the larger *J'* value in **6**·2H_2O was not reproduced in its zinc analogue. Short side-on NO···NO contacts in crystalline nitroxyl radicals[27] can be associated with intermolecular antiferromagnetic couplings of up to −100 cm^{-1}.[28] Hence, while it remains to be crystallographically confirmed, this larger *J'* might arise from a pairwise intermolecular NO···NO interaction in **6**·2H_2O, which would be modelled equally well by eq 1.

In conclusion, the magnetic structure of **6**·2H_2O is distinct from **1**-**5**, showing *ca* 4x larger couplings between the spins in the molecule. DF calculations show that can be explained by a sterically induced change in the Jahn-Teller structure of the copper ion in $\mathbf{6}^{2+}$ towards structure B (Chart 1), with a $\{d_{z2}\}^1$ ground state.[2,3,9] Our current work aims to design new switchable heterospin molecular magnets based on this concept.

Experimental data sets associated with this paper are available from the University of Leeds library (http://doi.org/10.5518/591).

ASSOCIATED CONTENT

Supporting Information

The Supporting Information is available free of charge on the ACS Publications website at DOI: 10.1021/acs.inorgchem.
########.

Experimental procedures for the synthesis, physical and computational characterization of the complexes; crystallographic Figures and tables; additional magnetic susceptibility data; computed structures and orbital plots; and, discussion and calibration of the computed *J* values (PDF).

X-ray crystallographic data in CIF format (CIF).

Accession Codes

CCDC 1911909 and 1911991 contain the supplementary crystallographic data for this paper. These data can be obtained free of charge via www.ccdc.cam.ac.uk/data_request/cif, or by emailing data_request@ccdc.cam.ac.uk, or by contacting The Cambridge Crystallographic Data Centre, 12 Union Road, Cambridge CB2 1EZ, UK; fax: +44 1223 336033.

AUTHOR INFORMATION

Corresponding Authors

Stephen Sproules – WestCHEM, School of Chemistry, University of Glasgow, Glasgow G12 8QQ, UK;
Email: stephen.sproules@glasgow.ac.uk.

Victor I. Ovcharenko – International Tomography Center SB RAS, Institutskaya str. 3a, 630090 Novosibirsk, Russia;
Email: victor.ovcharenko@tomo.nsc.ru.

Malcolm A. Halcrow – School of Chemistry, University of Leeds, Woodhouse Lane, Leeds LS2 9JT, UK; Department of Chemistry, Graduate School of Science, Osaka University, Toyonaka, Osaka 560-0043, Japan;
Email: m.a.halcrow@leeds.ac.uk.

Authors

Sam Greatorex – School of Chemistry, University of Leeds, Woodhouse Lane, Leeds LS2 9JT, UK.

Sergey V. Fokin – International Tomography Center SB RAS, Institutskaya str. 3a, 630090 Novosibirsk, Russia.

Rafal Kulmaczewski – School of Chemistry, University of Leeds, Woodhouse Lane, Leeds LS2 9JT, UK.

Mihoko Yamada – Department of Chemistry, Graduate School of Science, Osaka University, Toyonaka, Osaka 560-0043, Japan; Division of Materials Science, Graduate School of Science and Technology, Nara Institute of Science and Technology, Ikoma, Nara 630-0192, Japan.

Oscar Cespedes – School of Physics and Astronomy, University of Leeds, EC Stoner Building, Leeds LS2 9JT, UK.

Nobuto Yoshinari – Department of Chemistry, Graduate School of Science, Osaka University, Toyonaka, Osaka 560-0043, Japan.

Takumi Konno – Department of Chemistry, Graduate School of Science, Osaka University, Toyonaka, Osaka 560-0043, Japan.

Notes

The authors declare no competing financial interests.

ACKNOWLEDGMENTS

This work was funded by the Royal Society (IE150010), EPSRC (EP/K012576/1, EP/K00512X/1 and EP/M506552/1), CREST (JST JPMJCR13L3) and RSF (18-13-00380). MAH thanks Osaka University Graduate School of Science for a visiting appointment.

REFERENCES

(1) Halcrow, M. A. Jahn-Teller Distortions in Transition Metal Compounds, and their Importance in Functional Molecular and Inorganic Materials. *Chem. Soc. Rev.* **2013**, *42*, 1784–1795.

(2) (a) Solanki, N. K.; McInnes, E. J. L.; Mabbs, F. E.; Radojevic, S.; McPartlin, M.; Feeder, N.; Davies, J. E.; Halcrow, M. A. Steric Control of the Electronic Ground State in Six-Coordinate Copper(II) Complexes. *Angew. Chem. Int. Ed.* **1998**, *37*, 2221–2223. (b) Solanki, N. K.; Leech, M. A.; McInnes, E. J. L.; Zhao, J. P.; Mabbs, F. E.; Feeder, N.; Howard, J. A. K Davies, J. E.; Rawson, J. M.; Halcrow, M. A. The Effects of Distal Ligand Substitution on the Copper(II)/Bis-(2,6-Dipyrazol-1-yl-pyridine) Centre. *J. Chem. Soc. Dalton Trans.* **2001**, *2001*, 2083–2088.

(3) Holland, J. M.; Liu, X.; Zhao, J. P.; Mabbs, F. E.; Mabbs,; Kilner, C. A.; Thornton-Pett, M.; Halcrow, M. A. Copper Complexes of 2,6-Bis(iminomethyl)pyridine Derivatives and of 1,3-Bis-(pyridin-2-yl)pyrazole. Effects of Ligand Bulk and Conformational Strain on the Ground State of a Six-Co-ordinate Copper(II) Ion. *J. Chem. Soc. Dalton Trans.* **2000**, *2000*, 3316–3324.

(4) (a) Halcrow, M. A.; Kilner, C. A.; Wolowska, J.; McInnes, E. J. L.; Bridgeman, A. J. Temperature Dependence of the Electronic Ground States of Two Mononuclear, Six-Coordinate Copper(II) Centres. *New J. Chem.* **2004**, *28*, 228–233 and **2004**, *28*, 887 (correction). (b) Kilner, C. A.; Halcrow, M. A. Change in Electronic Structure in a Six-Coordinate Copper(II) Complex Accompanied by an Anion Order/Disorder Transition. *Acta Cryst., Sect. B: Struct. Sci.* **2010**, *66*, 206–212.

(5) Docherty, R.; Tuna, F.; Kilner, C. A.; McInnes, E. J. L.; Halcrow, M. A. Suppression of the Jahn-Teller Distortion in a Six-Coordinate Copper(II) Complex by Doping it into a Host Lattice. *Chem. Commun.* **2012**, *48*, 4055–4057.

(6) The ground states of structures A and A' are written as $\{d_{x2-y2}\}^1$ for simplicity. However, a more accurate notation in this symmetry is $\{d_{y2-z2}\}^1$, because the pseudo-Jahn-Teller elongation in structures A and A' does not lie on the unique symmetry axis (*z*) of the molecule.

(7) (a) Hitchman, M. A. The Influence of Vibronic Coupling on the Spectroscopic Properties and Stereochemistry of Simple 4- and 6-Coordinate Copper(II) Complexes. *Comments Inorg. Chem.* **1994**, *15*, 197–254. (b) Murphy, B.; Hathaway, B. The Stereochemistry of the Copper(II) Ion in the Solid-State – Some Recent Perspectives Linking the Jahn-Teller Effect, Vibronic Coupling, Structure Correlation Analysis, Structural Pathways and Comparative X-Ray Crystallography. *Coord. Chem. Rev.* **2003**, *243*, 237–262.

(8) (a) Folgado, J. V.; Henke, W.; Allmann, R.; Stratemeier, H.; Beltrán-Porter, D.; Rojo, T.; Reinen, D. Fluxionality in Hexacoordinated Copper (II) Complexes with 2,2':6',2"-Terpyridine (terpy) and Related Ligands: Structural and Spectroscopic Investigations. *Inorg. Chem.* **1990**, *29,* 2035–2042. (b) Meyer, A.; Schnakenburg, G.; Glaum, R.; Schiemann, O. (Bis(terpyridine))copper(II) Tetraphenylborate: a Complex Example for the Jahn-Teller Effect. *Inorg. Chem.* **2015**, *54*, 8456–8464.

(9) While structure B resembles a Jahn-Teller compressed geometry, this is impossible for **1**-**6** in the C_{2v} point group where the d_{z2} orbital is not degenerate by symmetry. A better description is that structure B represents suppression of the pseudo-Jahn-Teller elongation in structures A and A'.[1]

(10) (a) Fedin, M. V.; Veber, S. L.; Bagryanskaya, E. G.; Ovcharenko, V. I. Electron Paramagnetic Resonance of Switchable Copper-Nitroxide-Based Molecular Magnets: an Indispensable Tool for Intriguing Systems. *Coord. Chem. Rev.* **2015**, *289–290*, 341–356. (b) Meng, X.; Shi, W.; Cheng, P. Magnetism in One-Dimensional Metal–Nitronyl Nitroxide Radical System. *Coord. Chem. Rev.* **2019**, *378*, 134–150.

(11) See *eg* (a) Ovcharenko, V. I.; Romanenko, G. V.; Maryunina, K. Yu.; Bogomyakov, A. S.; Goreli, E. V. Thermally Induced Magnetic Anomalies in Solvates of the Bis(hexafluoroacetylacetonate)copper(II) Complex with Pyrazolyl-Substituted Nitronyl Nitroxide. *Inorg. Chem.* **2008**, *47*, 9537–9552. (b) Romanenko, G. V.; Maryunina, K. Yu.; Bogomyakov, A. S.; Sagdeev, R. Z.; Ovcharenko, V. I. Relationship between the Thermally Induced Reorientations of Aromatic Solvate Molecules in Cu(hfac)$_2$–Nitroxide Breathing Crystals and the Character of the Magnetic Anomaly. *Inorg. Chem.* **2011**, *50*, 6597–6609. (c) Ovcharenko, V.; Fokin, S.; Chubakova, E.; Romanenko, G.; Bogomyakov, A.; Dobrokhotova, Z.; Lukzen, N.; Morozov, V.; Petrova, M.; Petrova, M.; Zueva, E.; Rozentsveig, I.; Rudyakova, E.; Levkovskaya, G.; Sagdeev, R. A Copper–Nitroxide Adduct Exhibiting Separate Single Crystal-to-Single Crystal Polymerization–Depolymerization and Spin Crossover Transitions. *Inorg. Chem.* **2016**, *55*, 5853–5861. (d) Dong, X.; Lorenc, M.; Tretyakov, E. V.; Ovcharenko, V. I.; Fedin, M. V. Light-Induced Spin State Switching in Copper(II)-Nitroxide-Based Molecular Magnet at Room Temperature. *J. Phys. Chem. Lett.* **2017**, *8*, 5587–5592. (e) Ovcharenko, V.; Romanenko, G.; Polushkin, A.; Letyagin, G.; Bogomyakov, A.; Fedin, M.; Maryunina, K.; Nishihara, S.; Inoue, K.; Petrova, M.; Morozov, V.; Zueva, E. Pressure-Controlled Migration of Paramagnetic Centers in a Heterospin Crystal. *Inorg. Chem.* **2019**, *58*, 9187–9194.

(12) See *eg* (a) Okazawa, A.; Hashizume, D.; Ishida, T. Ferro- and Antiferromagnetic Coupling Switch Accompanied by Twist Deformation around the Copper(II) and Nitroxide Coordination Bond. *J. Am. Chem. Soc.* **2010**, *132*, 11516–11524. (b) Okazawa, A.; Ishida, T. Spin-Transition-Like Behavior on One Side in a Nitroxide-Copper(II)-Nitroxide Triad System. *Inorg. Chem.* **2010**, *49*, 10144–10147. (c) Luneau, D. Coordination Chemistry of Nitronyl Nitroxide Radicals Has Memory. *Eur. J. Inorg. Chem.* **2020**, *2020*, 597–604.

(13) Ulrich, G.; Ziessel, R. Selective Synthesis of a Novel Family of Oligopyridine Based Imino-Nitroxide Biradicals Catalysed by Selenium Dioxide. *Tetrahedron Lett.* **1994**, *35*, 1215–1218.

(14) Oshio, H.; Watanabe, T.; Ohto, A.; Ito, T. A One-Dimensional Helical Copper(II) Imino Nitroxide. *Inorg. Chem.* **1997**, *36*, 1608–1610.

(15) Oshio, H.; Yamamoto, M.; Ito, T. Double Helical Assembly of Imino Nitroxyl Diradicals by Silver(I) Ions. *J. Chem. Soc. Dalton Trans.* **1999**, *1999*, 2641–2643.

(16) Oshio, H.; Yamamoto, M.; Ito, T.; Kawauchi, H.; Koga, N.; Ikoma. T.; Tero-Kubota, S. Experimental and Theoretical Studies on Ferromagnetically Coupled Metal Complexes with Imino Nitroxides. *Inorg. Chem.* **2001**, *40*, 5518–5525.

(17) Mitsumoto, K.; Shiga, T.; Nakano, M.; Nihei, M.; Nishikawa, H.; Oshio, H. Spin Canting in a Cobalt(II) Radical Complex with an Acentric Counter Anion. *Eur. J. Inorg. Chem.* **2008**, *2008*, 4851–4855.

(18) (a) Zhou, S. Y.; Li, T.; Li, X.; Sun, Y. Q.; Wang, Q. L.; Liao, D. Z.; Tian, L. Syntheses, Structures, and Magnetic Characterizations of Five Mn(II) and Co(II) Complexes Based on 2,6-Pyridyl-Substituted Nitronyl and Imino Nitroxide Radical. *Inorg. Chim. Acta* **2016**, *444*, 131–140. (b) Babailov, S. P.; Peresypkina, E. V.; Journaux, Y.; Vostrikova, K. E. Nickel(II) Complex of a Biradical: Structure, Magnetic Properties, High NMR Temperature Sensitivity and Moderately Fast Molecular Dynamics. *Sensors Actuators B: Chemical* **2017**, *239*, 405–412.

(19) Chen, J.; Song, Y.; Gao, D.-Z.; Liao, D.-Z.; Jiang, Z.-H.; Yan, S.-P. Magnetic Interactions in a New Heterospin Complex Involving Nitroxide Radical and Oxamido Bridged Copper(II). *J. Coord. Chem.* 2007, **60**, 929–936.

(20) Lanfranc de Panthou, F.; Luneau, D.; Musin, R.; Öhrström, L.; Grand, A.; Turek, P.; Rey, P. Spin-Transition and Ferromagnetic Interactions in Copper(II) Complexes of a 3-Pyridyl-Substituted Imino Nitroxide. Dependence of the Magnetic Properties upon Crystal Packing. *Inorg. Chem.* **1996**, *35,* 3484–3491.

(21) Luneau, D.; Rey, P.; Laugier, J.; Fries, P.; Caneschi, A.; Gatteschi, D.; Sessoli, R. Nitrogen-Bonded Copper(II)-Imino Nitroxide Complexes Exhibiting Large Ferromagnetic Interactions. *J. Am. Chem. Soc.* **1991**, *113*, 1245–1251

(22) See *eg* (a) Oshio, H.; Yamamoto, M.; Ito, T. Cyanide-Bridged Molecular Squares with Ferromagnetically Coupled dπ, dσ, and pπ Spin System. *Inorg. Chem.* **2002**, *41*, 5817–5820. (b) Tretyakov, E. V.; Eltsov, I. V.; Fokin, S. V.; Shvedenkov, Y. G.; Romanenko, G. V.; Ovcharenko, V. I. Synthesis of 2-Iminonitroxide-Substituted Phenols and Pyridine-3-Oles. Copper(II) Complexes with Imino Nitroxides Containing 2-Hydroxyphenyl Substituents *Polyhedron* **2003**, *22*, 2499–2514. (c) Li, L.; Liao, D.; Jiang, Z.; Mouesca, J.-M.; Rey, P. An Unprecedented Asymmetric End-On Azido-Bridged Copper(II) Imino Nitroxide Complex: Structure, Magnetic Properties, and Density Functional Theory Analysis. *Inorg. Chem.* **2006**, *45*, 7665–7670. (d) Allão Cassaro, R. A.; Friedman, J. R.; Lahti, P. M. Copper(II) Coordination Compounds with Sterically Constraining Pyrenyl Nitronyl Nitroxide and Imino Nitroxide. *Polyhedron* **2016**, *117*, 7–13.

(23) O'Connor, C. J. Magnetochemistry – Advances in Theory and Experimentation. *Prog. Inorg. Chem.* **2007**, *29*, 203–283.

(24) Hayakawa, K.; Shiomi, D.; Ise, T.; Sato, K.; Takui, T. Stable Iminonitroxide Biradical in the Triplet Ground State. *Chem. Lett.* **2004**, *33*, 1494–1495.

(25) Shiomi, D.; Ito, K.; Nishizawa, M.; Hase, S.; Sato, K.; Takui, T.; Itoh, K. Charged Nitronyl Nitroxide Biradicals as Building Blocks for Molecular Ferrimagnetics. *Mol. Cryst. Liq. Cryst.* **1999**, *334*, 99–108.

(26) Francese, G.; Romero, F. M.; Neels, A.; Stoeckli-Evans, H.; Decurtins, S. Crystal Structures and Magnetic Properties of Metal Complexes Bearing Four Nitronyl Nitroxide Moieties in the Same Coordination Sphere. *Inorg. Chem.* **2000**, *39*, 2087–2095.

(27) Fedin, M. V.; Veber, S. L.; Maryunina, K. Yu.; Romanenko, G. V.; Suturina, E. A.; Gritsan, N. P.; Sagdeev, R. Z.; Ovcharenko, V. I.; Bagryanskaya, E. G. Intercluster Exchange Pathways in Polymer-Chain Molecular Magnets Cu(hfac)$_2$L^R Unveiled by Electron Paramagnetic Resonance. *J. Am. Chem. Soc.* **2010**, *132*, 13886–13891.

(28) See *eg* (a) Fettouhi, M.; El Ali, B.; El-Ghanam, A. M.; Golhen, S.; Ouahab, L.; Daro, N.; Sutter, J.-P. Temperature Dependence of the Crystal Lattice Organization of Coordination Compounds Involving Nitronyl Nitroxide Radicals: a Magnetic and Structural Investigation. *Inorg. Chem.* **2002**, *41*, 3705–3712. (b) Matsumoto, S.; Higashiyama, T.; Akutsu, H.; Nakatsuji, S. A Functional Nitroxide Radical Displaying Unique Thermochromism and Magnetic Phase Transition. *Angew. Chem. Int. Ed.* **2011**, *50*, 10879–10883. (c) Vaz, M. G. F.; Allão, R. A.; Akpinar, H.; Schlueter, J. A.; Santos, S. jr.; Lahti, P. M.; Novak, M. A. Magnetic Mn and Co Complexes with a Large Polycyclic Aromatic Substituted Nitronylnitroxide. *Inorg. Chem.* **2012**, *51*, 3138–3145. (d) Pang, X.; Zhao, X. R.; Wang, H.; Sun, H.-L.; Jin, W. J. Modulating Crystal Packing and Magnetic Properties of Nitroxide Free Radicals by Halogen Bonding. *Cryst. Growth Des.* **2013**, *13*, 3739–3745. (e) Maryunina, K.; Yamaguchi, K.; Nishihara, S.; Inoue, K.; Letyagin, G.; Romanenko, G.; Barskaya, I.; Veber, S.; Fedin, M.; Bogomyakov, A.; Petrova, M.; Morozov, V.; Ovcharenko, V. Intermolecular Spin-Crossover-like Phenomenon Sensitive to Applied External Pressure in Heterospin Crystals. *Cryst. Growth Des.* **2020**, *20*, 2796–2802.